

A COMPARISON OF ADAPTIVELY EQUALIZED PCM/FM, SOQPSK, AND MULTI-H CPM IN A MULTIPATH CHANNEL

**Terrance Hill & Mark Geoghegan
Nova Engineering Inc., Cincinnati, OH**

ABSTRACT

It is widely recognized that telemetry channels, particularly airborne channels, are afflicted by multipath propagation effects. It has also been shown that adaptive equalization can be highly effective in mitigating these effects. However, numerous other factors influence the behavior of adaptive equalization, and the type of modulation employed is certainly one of these factors. This is particularly true on modulations which exhibit different operating bandwidths. In this paper, we will examine the effect multipath and adaptive equalization for three modulation techniques which are either already in use, or have been proposed, for airborne telemetry.

KEY WORDS

Adaptive Equalization, Multipath, PCM, SOQPSK, Continuous Phase Modulation

INTRODUCTION

For many years, pulse code modulation / frequency modulation (PCM/FM) has been ubiquitous in the telemetry community. This binary modulation offers a number of advantages such as a constant envelope waveform, simple non-coherent detection, and inexpensive implementations at both ends of the link. Its utilization of spectrum,

however, is relatively inefficient and this has led to the development of new modulation techniques which offer more data capacity in less bandwidth. Although these new waveforms are highly effective in this regard, there is cause for concern about their performance in a multipath environment. These concerns arise precisely because the modulations use less spectrum. Because a multipath channel creates spectral nulls in the transmission function of the channel, intuition would suggest that a modulation technique which concentrates its energy in a narrower band would be more susceptible to degradation by the multipath-induced spectral notches. Our purpose here is to explore this effect quantitatively. In addition to evaluating the effect of multipath distortion, we will analyze the extent to which practical adaptive equalizers can mitigate multipath.

THE WAVEFORMS

Several excellent papers have been published describing the ARTM waveforms, so we will only briefly describe them here. For the sake of simplicity, we will refer to the legacy PCM/FM waveform as ARTM Tier 0, even though this technique has been in use since long before the ARTM program was launched. (The enhanced multi-symbol demodulator for this waveform, however, was developed under the ARTM program, so it's not unreasonable to call it the ARTM Tier 0 demodulator.) When we refer to Tier I waveforms, we will mean either FQPSK-B or SOQPSK, as these modulations are interoperable, and essentially indistinguishable. The Tier II waveform refers to the particular variant of multi-h continuous phase modulation (CPM) which has been implemented under the ARTM program.

Table 1 summarizes the key features of these three waveforms, and their time domain and frequency domain characteristics are depicted in Figure 1.

| | PCM/FM (Tier 0) | SOQPSK (Tier 1) | Multi-h CPM (Tier 2) |
|--|--------------------------|----------------------------|--------------------------|
| Bandwidth Efficiency relative to PCM/FM | 1x | 2x | 3x |
| Link Margin relative to conventional PCM/FM | 3 dB | 0 dB | 0 dB |
| Compatibility | Existing transmitters | Compatible with FQPSK-B | Ideal for new designs |

Table 1. Key features of PCM/FM, SOQPSK, and Multi-h CPM.

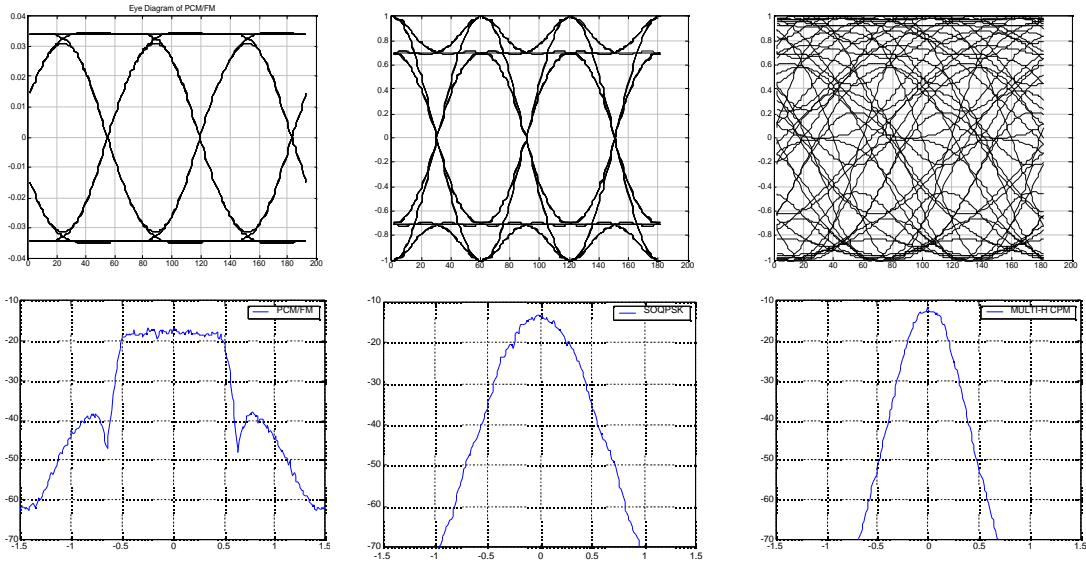


Figure 1. Time- and frequency-domain characteristics of PCM/FM (left), SOQPSK (center), and Multi-h CPM (right).

THE CHANNEL

The multipath channel being modeled here is a simple two-ray configuration, with a complex reflection coefficient, ρ . Therefore the impulse response of the channel is given by

$$h(t) = 1.0 * \delta(t) + \rho * \delta(t-\tau)$$

where $\delta(t)$ is the unit impulse function, and the frequency response is given by

$$H(\omega) = 1 + \rho * e^{-j\omega\tau}$$

Such a channel has a periodic frequency response, with a period of $2\pi / \tau$ radians per second, and a peak-to-null amplitude ripple (in dB) of $20 \log ((1 + |\rho|) / (1 - |\rho|))$. The phase angle of ρ affects only the shift of the response on the frequency axis. For the range of data rates and channel delays of interest here, there is typically only a single null present in the bandwidth of the signal spectrum.

As an example, the magnitude response of the channel $h(t) = 1.0 * \delta(t) + (0.632 + j0.632) * \delta(t - 1.0 T_b)$, where T_b is the bit period, is shown in Figure 2.

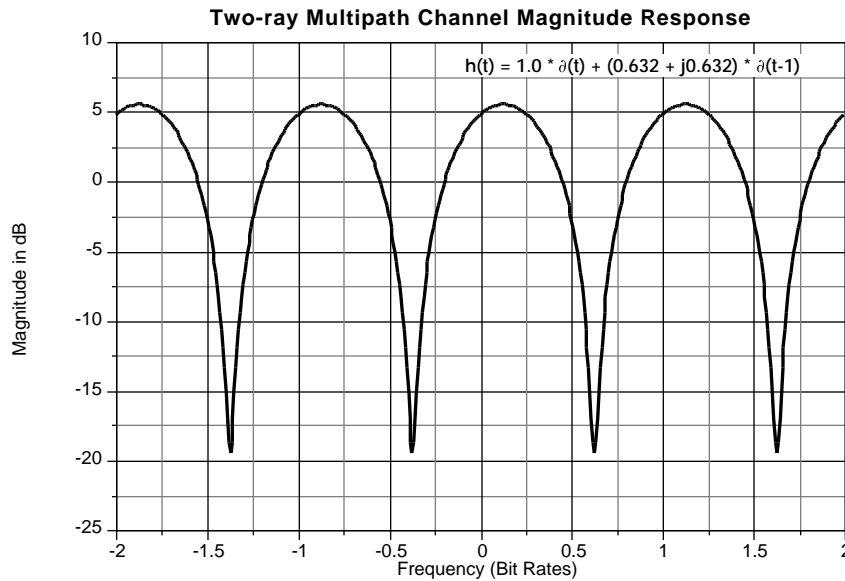


Figure 2. Typical Multipath Channel Response.

THE EQUALIZER

Previous research has shown that the constant modulus algorithm (CMA) is quite effective against multipath, particularly for constant-envelope signals, such as those under consideration here. The CMA has the advantage of being able to operate without a training sequence, even if the multipath is severe enough to close the eye pattern in the demodulator. This is in contrast to the least mean squares (LMS) algorithm, which although it can provide smaller mean squared error, will only converge to a solution when under moderate channel distortion, unless periodic training sequences are interspersed into the data stream.

The CMA equalizer modeled here is depicted in Figure 3. Note that the error signal used to drive the adaptive taps consists only of the deviation of the signal from the unit circle. In other words, the algorithm seeks only to restore the signal to the unit circle. Since all of the modulations under investigation here are constant envelope waveforms, this constitutes a "fair" error metric for all three modulations.

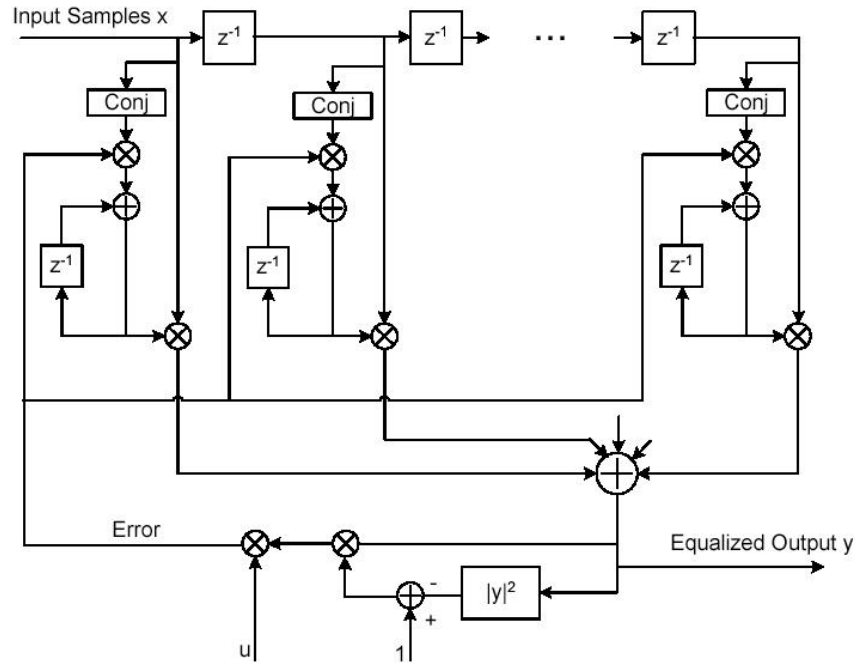


Figure 3. Block Diagram for CMA Equalizer.

The acquisition performance of the equalizer was investigated in some detail, but we will only briefly summarize those results in this paper. A representative example of the acquisition performance is shown in Figure 4. The unequalized signal for this channel exhibited an error of about -5 dB, and after a few thousand symbols to converge the taps, the CMA was able to reduce this error by about 20 dB. For this channel, the LMS algorithm, was able to provide somewhat greater improvement, but as discussed above, the CMA will converge without training under conditions when the LMS algorithm will not.

Once we had determined that the convergence behavior of the equalizer was robust over a broad range of channel characteristics, we elected to shorten the simulation times by initializing the equalizer taps to the optimum taps, w_0 , given by the Weiner-Hopf equation, i.e., $w_0 = R^{-1} p$, where R is the autocorrelation matrix of the equalizer input vector and p is the cross-correlation vector between the input vector and the desired (ideal) output vector. Initializing the taps to w_0 had the effect of treating the equalizer as if it had been given a very long time to converge, while the channel remained static. It will be the topic of another paper to report on the acquisition and tracking behavior of the taps under dynamic fading conditions.

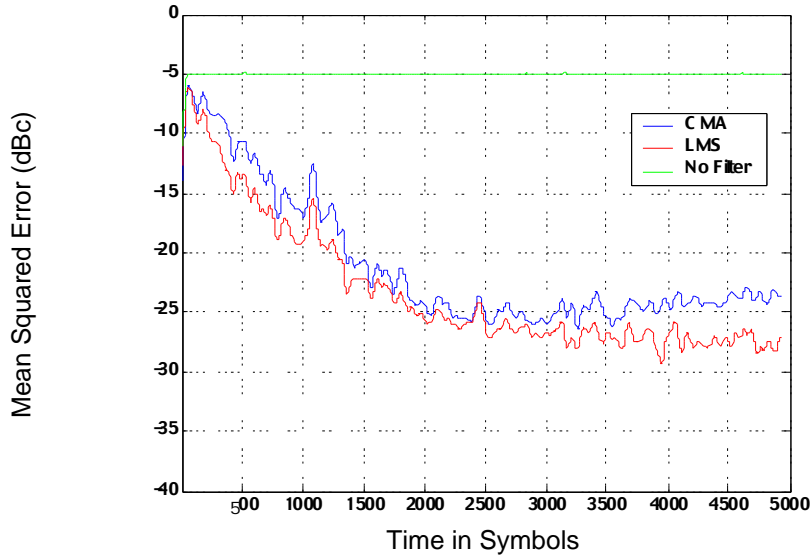


Figure 4. Simulated acquisition performance of both CMA and Least Mean Square (LMS) algorithms.

ANALYTICAL METHOD

In this section, we will describe the method by which the results presented below were derived. A block diagram of the experimental technique is shown in Figure 5. The source signals used were the ARTM Tier 0, Tier 1, and Tier 2 waveforms as defined above. The modulated waveform was distorted by the static two-ray multipath channel, and then white Gaussian noise was added. The AWGN had the effect of keeping the initialization of the equalizer taps from being "more optimum" than would actually be possible in the presence of noise.

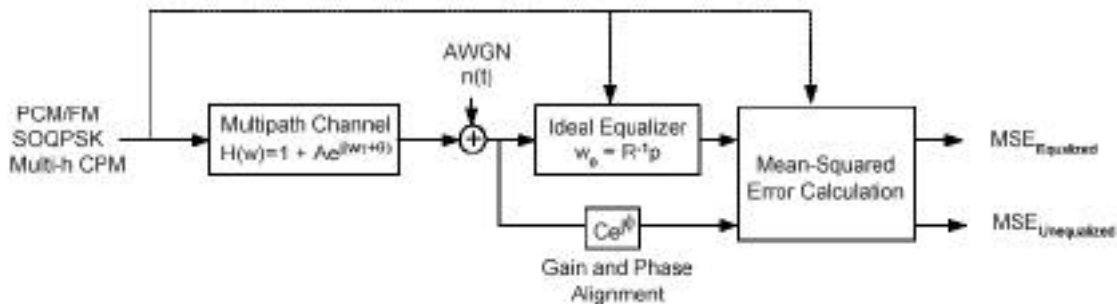


Figure 5. Block Diagram of Equalizer Evaluation Experiment.

The mean squared error (MSE) of the equalizer output was calculated as follows. Both the ideal, undistorted waveform and the equalizer output were treated as a complex-

valued signal vectors. The MSE is then simply given by the average of the square of the Euclidian distance between the corresponding vector elements. Note that, while this method provides a common frame of reference for all three modulations, we have not analyzed the relationship between MSE and other performance metrics such as bit error rate (see Future Work section).

PERFORMANCE RESULTS

The experiment defined above describes a multi-dimensional parameter space. The key factors affecting overall performance are three values which define the multipath channel (second-path delay and the magnitude and phase of the reflection coefficient), two numbers which define the equalizer (number of taps and tap spacing), an assumed Gaussian signal to noise ratio, and the choice of one of the three modulation techniques. Even with only these seven parameters, a complete mapping of the space is clearly impractical. Consequently, we will present here a subset of interesting cases.

For all the results which follow, the magnitude of the reflection coefficient, ρ , is 0.894. Because the peak of the multipath channel response is given by $1 + |\rho|$, and the minimum is given by $1 - |\rho|$, this value of ρ creates a max to min channel variation of 25 dB. The signal to noise ratio (E_b/N_0) for the results presented here is 35 dB, and the equalizer always has 32 complex-valued taps.

One of the first stages of the analysis was to explore performance as a function of equalizer tap spacing. Under our constraint that the equalizer is limited to 32 taps, the tap spacing and total equalizer span are inversely related. In Figure 6, we show some typical results for a multipath notch at the center of the signal spectrum. Examination of this figure shows that for any particular configuration, there is an optimum tap spacing. As our goal in this research is to develop and implement a practical equalizer for telemetry applications, we are strongly motivated to use the same tap spacing for all conditions. The results in Figure 6 steered us to use four samples per symbol, or a tap spacing of $T_s/4$. Using fewer samples per symbol causes performance to degrade because the equalizer is unable to resolve the separate multipath components. At the opposite extreme, using 8 or 16 samples per symbol causes the equalizer span to be too short to fully correct for the longer multipath delays. A tap spacing of $T_s/4$ is a good compromise over a reasonably broad range of data rates and second-path delays. All of the remaining results are for equalizers operating at four samples per symbol.

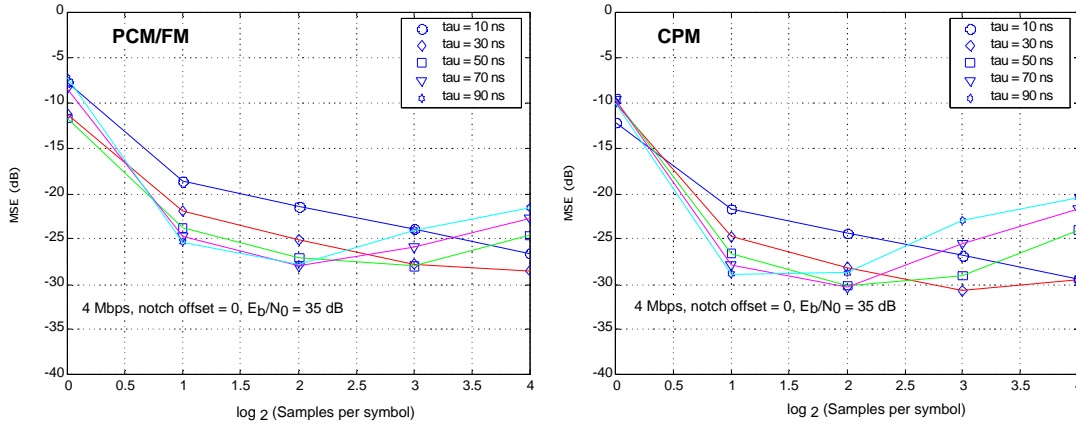


Figure 6. MSE as a Function of Tap Spacing, 4 Mbps, 25 dB Notch at Center.

Figures 7 and 8 show the effectiveness of the equalizer for all three modulations, at four data rates, five different second-path delays, and various offsets between the carrier and the multipath-induced spectral notch. As discussed above, there are a number of interrelated parameters in this analysis, and it is not practical to explore all possible combinations. Figures 7 and 8 are representative examples.

From top to bottom in these figures, the modulation changes from PCM/FM, to SOQPSK, to CPM. Left to right, the data rate steps through 2, 4, 8, and 16 Mbps. Examining these twelve plots as a set, several observations are in order. First of all, for all cases, the equalizer is very effective in reducing the MSE of the multipath-distorted waveform. The unequalized MSE is generally in the range of -7 dB to -15 dB for this channel, while the MSE at the equalizer output is most often in the range of -20 dB to -35 dB; this is a significant improvement. Note that because the analysis was performed at $E_b/N_0 = 35$ dB, the smallest the MSE could ever be is -35 dB for PCM/FM and -38 dB for the two 4-ary modulations. We see that there are a number of points in the equalized plots which are within only a few dB of this asymptotic bound.

Figure 9 shows the improvement in MSE provided by the equalizer, computed simply as the difference between the unequalized and equalized MSE curves. For all three modulations, we see that the equalizer offers the most improvement when the notch is centered on the carrier. We also see that there are two domains where the improvement is more modest: short delays at low data rates, and long delays at high data rates. This behavior is best explained as follows. At low data rates (long symbols), the short delays are significantly less than the $T_s/4$ tap spacing. Consequently the equalizer does not have enough sampling resolution to separate the two copies of the signal, and as the delays get

shorter, this failing becomes more significant. For example, at 2 Mbps with the 4-ary modulations, $T_s/4$ is 250 nS. All of the delays considered here are significantly less than this, so the equalizer is hampered by the lack of sampling resolution, more so as the delays get shorter.

At the opposite extreme, high data rates with long delays, the equalizer span is shorter than required for optimum performance. Our 32-tap equalizer, with $T_s/4$ spacing, has a total span of 8 symbols. Consider PCM/FM at 16 Mbps. For this case, the equalizer span is 500 nS, which is less than 6 times the longest delay analyzed here, 90 nS. With these combinations of high data rates and longer delays, the equalizer's effectiveness is limited by total span. Naturally, this limitation becomes more significant as the data rate increases.

Comparing the two 4-ary modulations (SOQPSK and CPM), we see that the MSE is very similar in nearly all cases. Most of the differences in performance between SOQPSK and CPM can be understood by considering their respective spectral characteristics. CPM has the narrower spectrum; hence, we would expect it to be more degraded than SOQPSK when the multipath notch is near the carrier frequency, but less so in those cases where the spectral nulls essentially "straddle" the signal spectrum. This effect is seen most readily at the maximum data rate (16 Mbps, $T_s = 125$ nS) and longest delay (90 nS). Comparing the plots for SOQPSK and CPM, we see that CPM incurs more degradation than SOQPSK when the notch is within 0.5 bit rates of the carrier, but vice versa outside that range (when the multipath notches straddle the spectrum).

CONCLUSIONS

The objective of this analysis was to quantify the effectiveness of adaptive equalization for the ubiquitous PCM/FM waveform, as well as the emerging ARTM Tier 1 and Tier 2 waveforms. Within the limitations of the analytical method (see Future Work, below), we have shown that a CMA adaptive equalizer can be very effective against the multipath channels typically encountered in airborne telemetry applications. We have shown that for the range of data rates of most interest, a tap spacing of $T_s/4$ is a good choice. If the application includes very short delays or lower data rates, then using more samples per symbol is beneficial, although performance against long delays or at higher data rates will suffer. Although not explicitly presented here, all our results indicate that increasing the number of equalizer taps expands the region of effectiveness in both data rate and differential delay.

Overall, we conclude that the superior spectral efficiency of the ARTM Tier 1 and Tier 2 waveforms does not necessarily doom them to be more vulnerable to multipath than PCM/FM, if adaptive equalization is employed. However, we also recognize that although these results are encouraging, they are not complete. Next steps are discussed briefly in the following section.

FUTURE WORK

There are a number of embedded assumptions in the work presented here. A more thorough treatment of this topic necessarily involves a relaxation, or at least a re-examination, of these assumptions. We hope to present additional results in future papers which address these issues:

- Relationship of MSE to BER – The results presented here express the equalizer effectiveness in terms of mean squared error. However, multipath distortion does not look like AWGN, so inferring a bit error rate based on MSE is problematic. Measured data from real hardware will be used to quantify this relationship.
- Demodulator synchronization – A significant aspect of system performance is the acquisition and tracking of the demodulator's carrier and timing recovery loops. This is another area in which measured data from real hardware is most convincing, and we plan to employ this approach in future work.
- Two-ray multipath model – Several excellent papers have shown that a three-ray model offers a better representation of real channels. This also an area which we hope to explore with actual hardware.
- Channel dynamics – We have assumed in these results that the channel is static. Future results will explore how performance changes under dynamic channel conditions. In particular, the interaction of channel dynamics with equalizer tracking and demodulator synchronization calls for more research.
- Acquisition behavior – The initialization of the taps to w_0 using the Weiner-Hopf equation is a convenient shortcut, but clearly represents an ideal performance bound. Further analysis is required to determine the extent to which actual acquisition deviates from this optimum solution.
- Static taps – In the results presented here, the equalizer taps are initialized with the Weiner-Hopf equation and left fixed. Again, this represents a performance bound, but additional work is required to explore the effect of allowing the taps to vary dynamically.

ACKNOWLEDGEMENTS

The authors wish to express their appreciation to Kip Temple of AFFTC, Edwards AFB, Bob Jefferis of Tyrbine Corp., Gene Law of NAWCWD, Point Mugu, CA and Dr. Michael Rice of Brigham Young University, all of whom have offered insights on multipath channels, demodulator dynamics, and other aspects of the work presented here.

REFERENCES

1. T. Hill, "An Enhanced, Constant Envelope, Interoperable Shaped Offset QPSK (SOQPSK) Waveform for Improved Spectral Efficiency", Proceedings of the International Telemetry Conference, San Diego, CA, October 2000.
2. E. Law, "Estimating the Characteristics of the Aeronautical Telemetry Channel during Bit Error Events", Proceedings of the International Telemetry Conference, Las Vegas, October 1999.
3. M. Rice, E. Law, "Aeronautical Telemetry Fading Sources at Test Ranges", Proceedings of the International Telemetry Conference, Las Vegas, October 1997.
4. M. Geoghegan, "Description and Performance Results for the Advanced Range Telemetry (ARTM) Tier II Waveform", Proceedings of the International Telemetry Conference, October 2000.
5. J.B. Anderson, T. Aulin, C.E. Sunberg, Digital Phase Modulation, Plenum Press, New York NY, 1986
6. I. Sasase, S. Mori, "Multi-h Phase Coded Modulation", IEEE Communications Magazine, Vol. 29, No. 12, December 1991
7. E. Law, K. Feher, "FQPSK Versus PCM/FM for Aeronautical Telemetry Applications; Spectral Occupancy and Bit Error Probability Comparisons", Proceedings of the International Telemetry Conference, Las Vegas, October 27-30, 1997
8. A. Premji, D.P. Taylor, "A Practical Receiver Structure for Multi-h CPM Signals", IEEE Trans. On Communications, Vol. Com-35, No. 9, September 1987
9. J.G. Proakis, Digital Communications, McGraw Hill Book Company, 1995

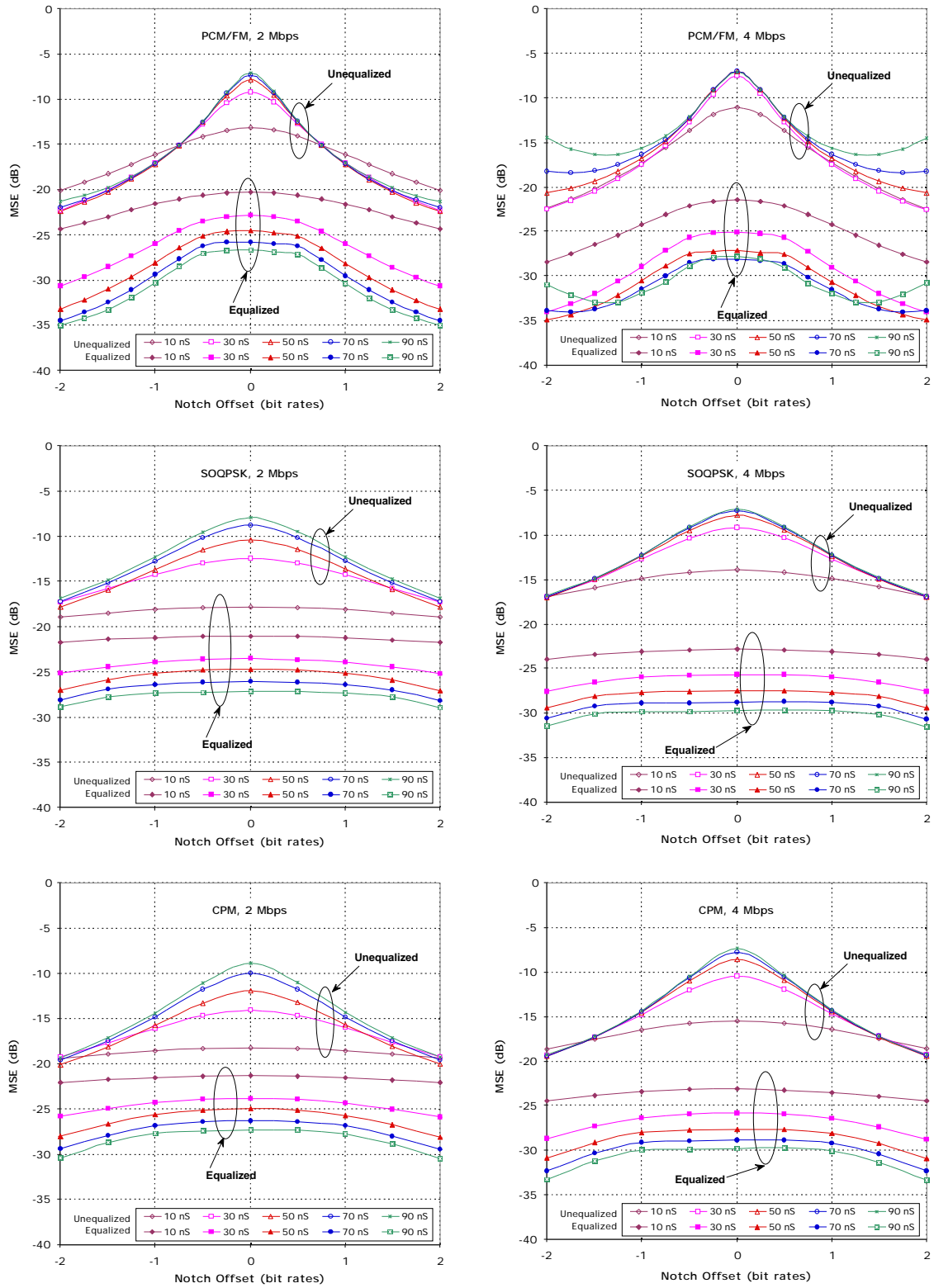


Figure 7. MSE as a Function of Notch Position, 2 Mbps and 4 Mbps.

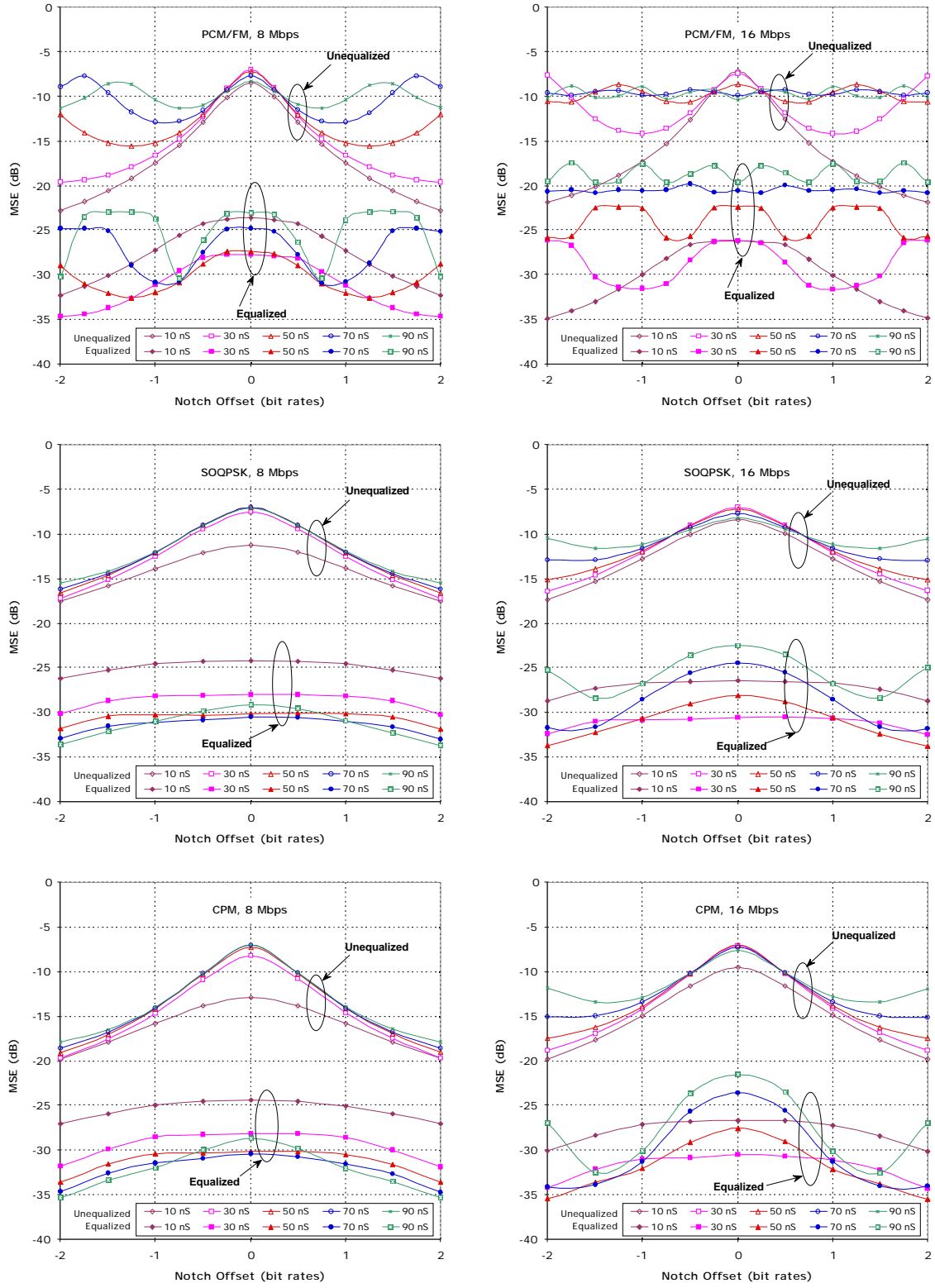


Figure 8. MSE as a Function of Notch Position, 8 Mbps and 16 Mbps.

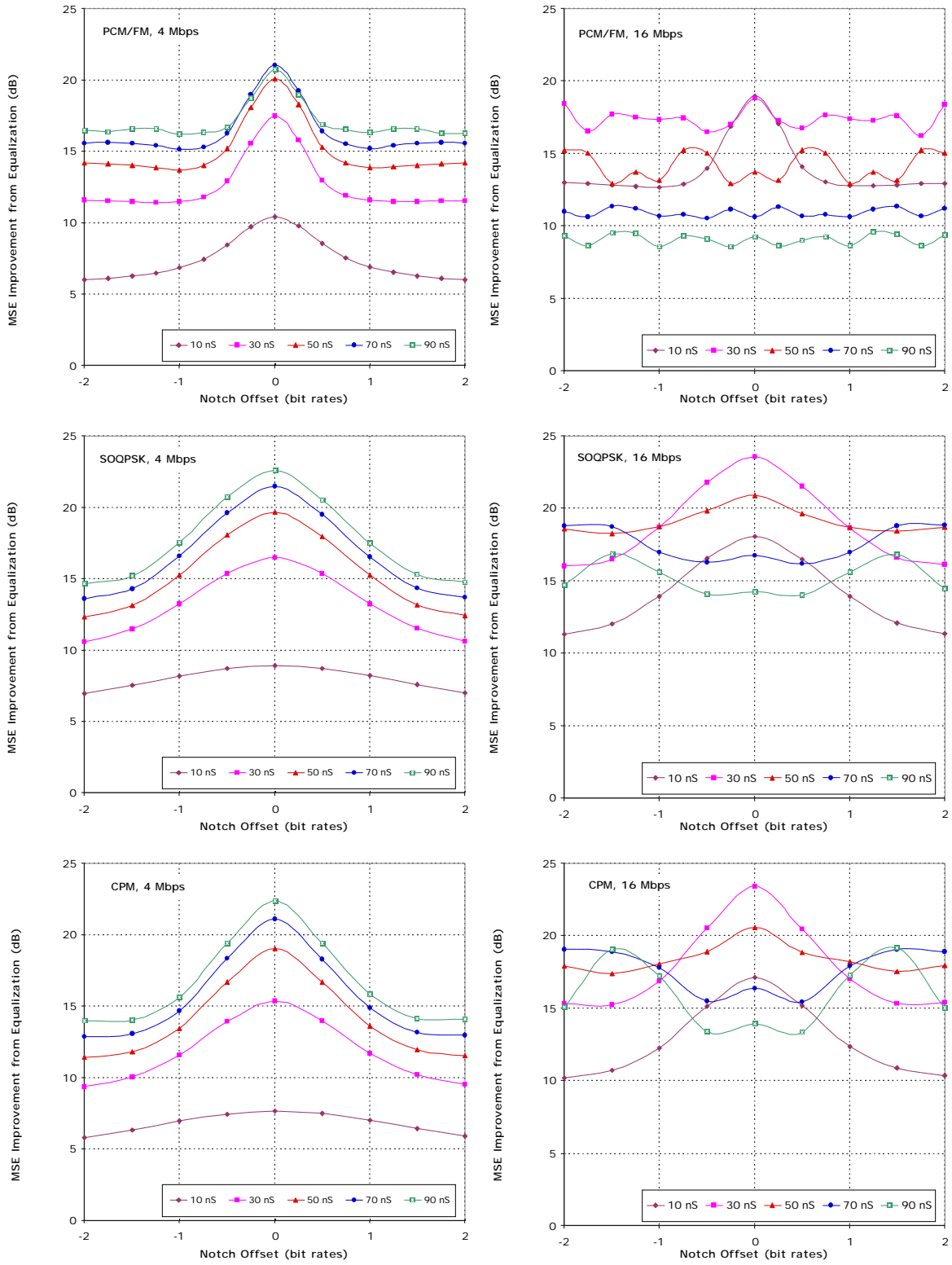


Figure 9. MSE Improvement as a Function of Notch Position, 4 Mbps and 16 Mbps.